SUBMILLIMETER AND FAR INFRARED EMISSION FROM SOLAR FLARES

VAHÉ PETROSIAN
CSSA, Stanford University, Stanford, CA 94305, U.S.A.

Abstract. The mechanisms for emission in the submillimeter and far-infrared (10^{11} and 10^{13} Hz) regions by solar flares and expected fluxes at these frequencies are described and evaluated. These inferences are based on observations of flare emission at other frequencies and on models for these emissions. In the impulsive phase, non-thermal synchrotron emission by electrons responsible for > 10 MeV gamma-ray emission can give rise to significant radiation in the 10^{11} to 10^{13} Hz region from large flares. Free-free or thermal gyrosynchrotron from the hot plasma responsible for the gradual soft X-ray emission can produce significant radiation in the 10^{11} to 10^{13} Hz range. However, only radiation in the lower end of this range would have a brightness temperature exceeding the quiet sun brightness.

Key words: infrared: stars – Sun: flares –Sun: particle emission – Sun: radio radiation – Sun: X-rays, gamma rays

1. Introduction

Electromagnetic radiation from solar flares has been observed from tens of MHz frequencies to GeV energies with a notable gap in the 10^{11} to 10^{14} Hz range. I will attempt to estimate the expected fluxes in this range concentrating on the lower end of this range, *i.e.* in the submillimeter and far infrared region (submm and FIR, respectively). Although I will not discuss such emissions from active regions, some of the extrapolations used here, especially those in connection with thermal emission, will be applicable to active regions as well.

In Section 2 I will present an overall description of the relevant observations. In Section 3 I will describe the general features of models which can successfully explain these features and indicate what the predictions of such models are for emission in the Submm and FIR range. In section 4 I will describe some recent observations and indicate how they can be extrapolated to predict the fluxes in Submm and FIR range. Finally, I will present a brief summary in section 5.

2. Overview of Flare Emission

Figure 1 shows a schematic spectrum of flare emission from 10^8 to 10^{24} Hz where I plot, as a function of the logarithm of frequency ν, the logarithm of the product of frequency and flux density, $F(\nu)$. The flare emission has been divided into two parts, which are usually referred to as "Impulsive" and "Gradual" phase emissions, typically lasting 1 to 100 seconds, and minutes to hours respectively. Such a division, of course, is not clearly defined and does not apply to all flares. A more clear distinction between these two phases, the one which I shall adopt here, is division by the type of radiation mechanism. By the Impulsive phase I will refer to non-thermal emission by accelerated electrons (accelerated ions will not be important in my discussion) while the Gradual phase will refer to thermal emission by plasma heated or evaporated as a result of energy deposition by accelerated particles or by other processes (such as plasma turbulence or shocks.)

D. M. Rabin et al. (eds.), Infrared Solar Physics, 103–112.

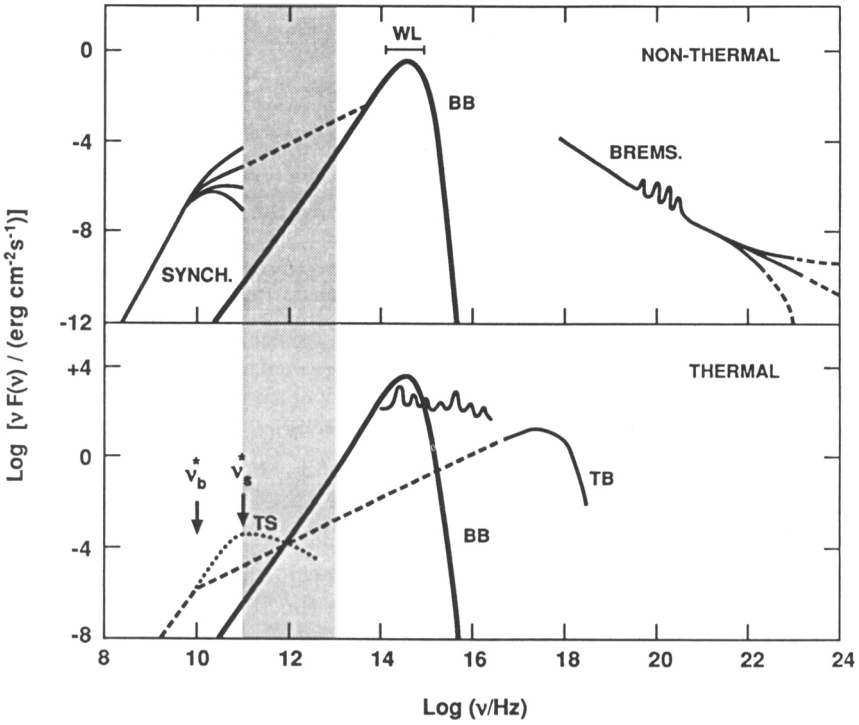

Fig. 1. A schematic presentation of typical strong solar flare spectra over a wide range of frequencies. The upper panel represents the impulsive phase, *i.e.* non-thermal emission, and the lower panel gradual thermal emission. Solid lines are observed, dashed and dotted lines are based on model extrapolations. The heavy solid line represent black body (BB) emission at 5800 K from 1 and 10^4 arcsec^2 area in the upper and lower panels, respectively. The wiggly portions indicate the presence of nuclear (upper panel) and atomic (lower panel) lines. WL stands for white-light emission.

It should also be noted that the relative and absolute values of fluxes shown in Figure 1 are very rough measures of the actual values. This is because, first, there is no such thing as a typical value of flux at any frequency. Distributions of fluxes obey power law forms extending over many decades whenever such distributions are available. Second, even though there is a strong correlation between emission at different frequencies, this correlation is only statistical in the sense that the distribution of flux ratio at different frequencies generally has a large dispersion. The solid lines in Figure 1 show observations for a relatively large flare. The dashed lines are extrapolations based on models described next.

3. Basic Models

It is generally believed that the source of energy of flares is the current-carrying magnetic field and that this energy is released by some reconnection mechanism.

https://doi.org/10.1017/S0074180900124325 Published online by Cambridge University Press

Observations require that a substantial fraction, if not all, of this energy goes into acceleration of electrons and ions either directly or via generation of plasma turbulence or shocks. If the plasma density is high in the acceleration region, some of this energy can be dissipated quickly and heat the plasma. The model which has become almost standard is that the bulk of accelerated particles are injected into a magnetic loop and that the interaction of these particles with the flare plasma in the loop produces the spectra shown in Figure 1. The interactions are many but the most important ones are interactions with large scale magnetic field geometry, Coulomb collision, synchrotron radiation at high energies (see *e.g.*, McTiernan and Petrosian 1990), and fairly uncertain but probably significant interactions with plasma turbulence (Miller and Ramaty 1989; Hamilton and Petrosian, 1992). For analyses of these processes one requires knowledge of the variation, along the length s of the loop, of the plasma density $n(s)$, the magnetic field $B(s)$, and the turbulence energy density $w(s)$. For analysis of spatially unresolved observations, *i.e.* those integrated over the whole loop, the significant parameters are the column depth, N_{tr}, from the acceleration region (presumably at the top of the loop) to the transition region, the field convergence $d\ln B/ds$ and the ratio of the turbulence energy to the magnetic field energy $8\pi w(s)/B^2$.

The primary radiation processes sometimes are not the same as the primary energy loss mechanisms. We now describe these for the two phases mentioned above.

3.1. Impulsive Phase Radiation

At the heart of the impulsive phase lies the *Hard X-ray Emission* ($\geq$ 20 KeV), which is believed to be due to thick-target bremsstrahlung emission by the accelerated electrons. The observed spectra can be fit to a power law $F(k) \propto k^{-\gamma}$ where $F(k)$ is the flux of photons (photons s^{-1} cm^{-2} keV^{-1}) at photon energy k. This implies an accelerated electron energy spectrum $f(E) \propto E^{-\gamma-1}$. This model for the hard X-ray emission seems to be consistent with most of the other observations, in addition to the spectrum. It can explain temporal variations (Kiplinger *et al.* 1984, Lu and Petrosian 1988), and the few available spatially resolved observations (Brown, Hayward and Spicer 1981; Leach and Petrosian 1983; see also Kundu and Woodgate 1986), and polarization observations (Leach, Emslie,and Petrosian 1985).

The *Gamma-ray emission* ($>$ 300 keV) is also partly due to electron bremsstrahlung and, in the one to seven MeV range, partly due to nuclear line excitation by protons and ions. Emission at >10 MeV has been observed for a few flares. This is also believed to be due to electron bremsstrahlung, although pion decay gamma-rays could also contribute at these energies. Observational results that support the bremsstrahlung model are the distribution of fluxes, spectral indices and particularly the variations of these distributions or their moments across the solar disk (see *e.g.*, Rieger *et al.* 1983; Vestrand *et al.* 1987). Such variations can be attributed to the anisotropy of the bremsstrahlung emission, which increases with increasing photon energies (Petrosian 1985). Consequently, the analysis of gamma-ray emission provides strong constraints on the model parameters (McTiernan and Petrosian 1991). An important feature of the gamma-ray observations which has significant bearing on the expected submm and FIR emission is the spectral flattening at

higher energies which implies similar flattening of the spectrum of accelerated electrons. This flattening is evident in the aforementioned statistical analysis but also is present in direct observations of the so-called electron-dominated events (Rieger and Marschhäuser 1991), and in the spectrum of electrons seen in the interplanetary medium (Dröger *et al.* 1989).

The third emission process is that in the *microwave range*, which is believed to be synchrotron emission with emissivity, $j(\nu) \propto \nu^{-\gamma/2}$, from the coronal portion of the loop, in contrast to hard X-ray and gamma-ray emission which are radiated mainly from the footpoints. The very close correlation between the microwave and hard X-ray fluxes is the primary evidence that the accelerated electrons responsible for X-ray and gamma-ray emission produce the microwave radiation as well. There have been many attempts to fit the simultaneous hard X-ray and microwave radiation to the thick target model. The references to, and discussion of, those studies can be found in Lu and Petrosian (1990), who show that such a fit is possible for loops with length $L \simeq 10^9$cm and with magnetic field $B \simeq 350$ to 600 G.

The energy E (in units of mc^2) of a relativistic electron emitting at frequency ν is

$$E \approx (300 \text{ G}/B)^{1/2}(\nu/10^9 \text{ Hz})^{1/2}. \quad (1)$$

At $B=$ 500 G electrons with $E \geq 8$ produce the highest frequency observed microwave radiation ($\sim 10^{11}$ Hz). These electrons produce bremsstrahlung gamma-rays of ≤ 4 MeV. It is, therefore, important to know the photon spectrum at > 4 MeV for prediction of emission at higher frequencies (10^{11} to 10^{13} Hz).

It should be noted that interpretation of the microwave emission is not as straightforward as that of the hard X-rays because microwaves are subject to various absorption processes and the geometry of the magnetic field plays an important role in their emission and absorption. At high frequencies where synchrotron emission in optically thin the spectrum is not well known and can have the different forms shown in Figure 1. These factors clearly will add to the uncertainties in prediction of fluxes in the submm and FIR range.

The *White light* emission (indicated as WL in Figure 1) is another radiative signature of the impulsive phase which, unfortunately, is not well understood. We shall, therefore, not discuss the relevance of this observation to possible submm and FIR emission.

3.2. Thermal Emission

As shown in Figure 1, primary thermal emission ranges from the optical (10^{14} Hz) to the soft X-ray region (≤ 10 keV). Most of this radiation is believed to be coming from a plasma heated and evaporated by the energy deposition of non-thermal electrons and ions. The yield of non-thermal electrons to bremsstrahlung radiation is small ($Y \simeq 10^{-5}$) so that most of the energy is deposited in the plasma via Coulomb collisions and is subsequently radiated during the thermal phase. Thus the total emission during this phase is considerably larger than that during the impulsive phase.

Given the observed thermal emission, we can extrapolate it to the FIR and submm region. The thermal plasma, responsible for the observed emission in the UV to X-ray range, can reach temperatures of 10^8 K, emitting thermal bremsstrahlung (free-free) and bound-bound and bound-free photons. The free-free emission at a few KeV can be extrapolated to the microwave range as shown by the dashed line in Figure 1. However, at these frequencies the competing process of thermal gyrosynchrotron emission could also be significant (dotted line). We shall return to this in the next section.

4. Some Recent Observations

As pointed out above, Submm and FIR emission during the impulsive non-thermal phase most likely will be due to synchrotron radiation by relativistic electrons. These particles also produce gamma rays. Therefore, the most direct information about the Submm–FIR range comes from observations of gamma-rays and from extrapolation of the millimeter observations at $\nu < 10^{11}$ Hz. Recently there have been some new instruments in operation which have extended the impulsive-phase observation into these regions.

4.1. Millimeter Observations

The first indications that there may be significant emission at millimeter (and Submm) wavelengths came from observations of flat microwave spectra in some flares (among which there were some strong ones). Attention was drawn to these kinds of bursts first by Ramaty and Petrosian (1972) and later by Kaufmann *et al.* (1986). Figure 2 shows some of these spectra. To my knowledge, the latter authors were the first to observe millimetric emission from flares. The flux in one flare observed by them (not shown in Figure 2) continues to rise and reaches its maximum at the highest frequency observed, 90 GHz.

More recently the Maryland group, using BIMA, has observed many flares at 86 GHz during the June 1991 campaign of the Max 91 program (Kundu *et al.* 1991). An excellent example of this work is presented in Figure 3 where it is shown that during the impulsive phase the time profile of 86 GHz radiation matches exactly that of gamma-rays detected by the BATSE instrument of Compton-GRO. In addition, there is significant 86 GHz emission after the impulsive phase with a slower time evolution similar to that of GOES soft X-ray emission. The post-impulsive radiation is from the heated plasma, the X-rays are from thermal bremsstrahlung emission, while the millimetric radiation comes from either thermal bremsstrahlung or thermal gyrosynchrotron emission. Some of the spectra observed by BIMA and other telescopes are also flat (White *et al.* 1992).

4.2. Gamma-ray Observations

Observations by the GRS instrument on SMM during cycle 21 were the first to provide information about gamma-ray emission at energies greater than 10 MeV. Flares with such emission show a strong concentration toward the limb of the sun (Rieger *et al.* 1983). Analysis of GRS observations of cycle 22 flares has revealed the

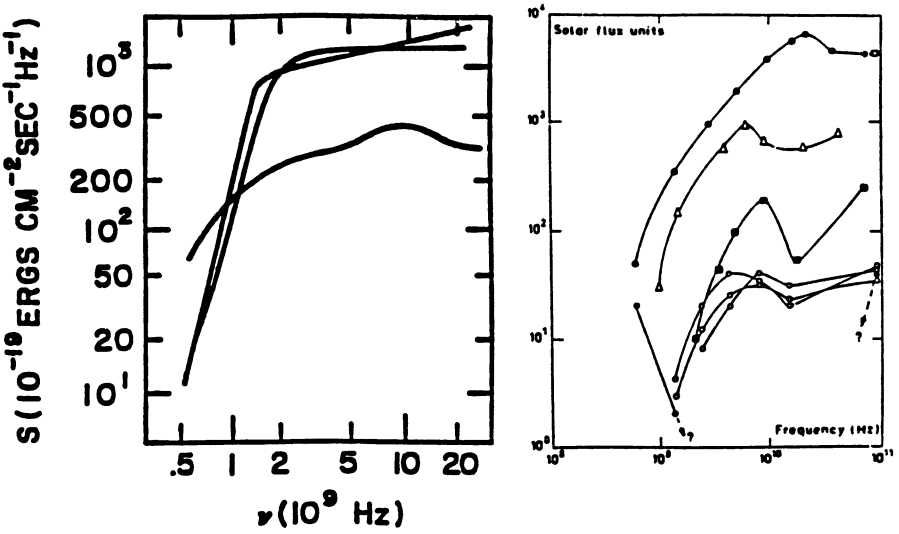

Fig. 2. Some examples of flat microwave spectra of flares. Left and right panels are from compilations by Ramaty and Petrosian (1972), and Kaufmann *et al.* (1986), respectively.

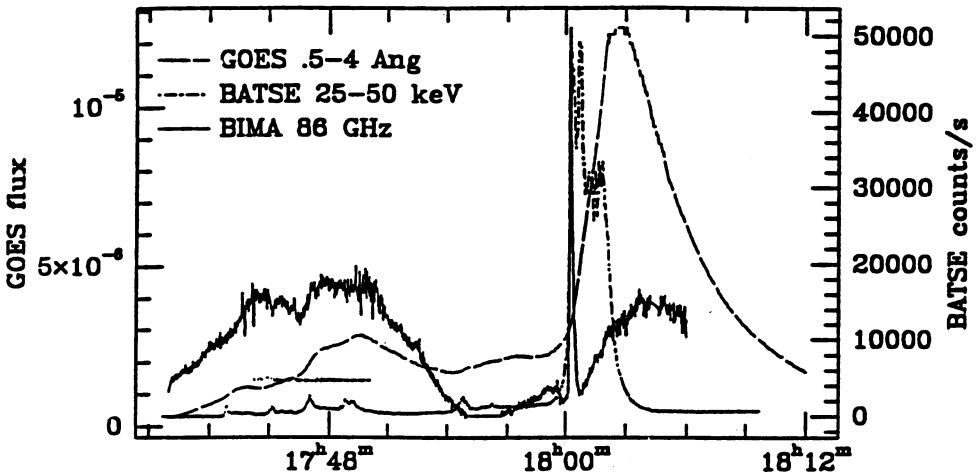

Fig. 3. The evolution of emission around 18 UT on 1991 June 13 seen in soft X-rays recorded by the GOES satellite (8 - 25 keV; long-dashed line), in 25 - 50 keV X-rays detected by BATSE (short-dashed line) and at 86 GHz recorded by BIMA (solid line). The gamma-ray (0.1 to 0.3 MeV) time profile by BATSE, not shown here, has also a single sharp spike coinciding with the first spike of hard X-ray (25 - 50 keV) and with the spike of the BIMA 86 GHz emission. The microwave peak flux is 6×10^{-19} erg/(cm^2 s Hz). [From Kundu *et al.*(1992).]

https://doi.org/10.1017/S0074180900124325 Published online by Cambridge University Press

existence of so-called electron dominated flares, which show no sign of nuclear line emission but a continuous emission up to ~50 MeV with a sharp drop-off beyond it (Rieger and Marschhäuser 1991). These suggest electron bremsstrahlung as a source of the high energy gamma-rays. The sharp cut-off at $\geq$50 MeV cannot be attributed to electron transport (synchrotron losses) or radiative transfer ($e^{\pm}$ pair production by gamma-rays) effects which become more important at higher photon energies. This cutoff must, therefore, reflect a steepening in the distribution of the accelerated electrons with $E > 10^2$ (Petrosian and McTiernan 1991). This indicates that we should expect synchrotron emission up to $\nu \approx 10^{13}(B/300G)Hz$.

The latest gamma-ray observation from the Gamma-1 instrument and from EGRET on Compton-GRO have shown flare emissions up to 1 or 2 GeV. Kocharov *et al.* 1991) interpret the Gamma-1 observation of the March 20, 1991 flare as due to electron bremsstrahlung and the June 15, 1991 flare as due to a combination of electron bremsstrahlung at low energies and π° decay at higher energies. The EGRET spectrum of the June 11, 1991 flare has spectral index $\gamma = 2.2$ and extends to 2 GeV. If this is an indication of the existence of electrons with energies > 100 MeV, we would expect synchrotron emission up to 10^{14} Hz. We should note that these and some of the flares observed by GRS in Cycle 22, unlike the flares with >10 MeV emission of Cycle 21, are not localized near the limb. This may be an indication of emission by π° decay which is expected to be more isotropic than electron bremsstrahlung. Alternatively, a pure electron bremsstrahlung model is possible if the magnetic field guiding the accelerated has a large non-radial component. In either case, whether the accelerated-electron spectrum is truncated at $\geq$ 100Mev or extends to 1 Gev, we expect synchrotron emission well into the Submm and FIR range.

4.3. Estimated Fluxes

As mentioned in the Introduction, the distribution of the observed fluxes of flares at all energies obeys a power law with no indication of a typical size. The Submm and FIR fluxes will most probably have similar distributions with most flares having fluxes at the instrumental threshold. In view of this, I now estimate the expected fluxes for some of the largest observed flares.

The *Impulsive Phase* fluxes can be estimated by either extrapolating the observed millimeter flares to higher frequencies or from consideration of the relative yield of synchrotron and bremsstrahlung radiation by relativistic electrons. These give similar results. In the first of these methods, the uncertainty lies in the spectral index one assumes in extending the fluxes to $\nu > 10^{11}$Hz. The flat spectrum flares shown in Figure 2 provide the best possibility of observing in the Submm and FIR range. The extrapolation to higher frequencies of these spectra depends on the model for such flat spectra. For a discussion of various possibilities see Ramaty and Petrosian (1973) and White *et al.* (1992).

Briefly, it seems unlikely that the flat spectra are produced by thermal bremsstrahlung. If the emission at higher frequencies is due to optically thin synchrotron emission, then the spectrum will depend on the spectral index of accelerated electrons. A flat spectrum would require a very hard electron spectrum ($\gamma \approx 0$ in

the thick target model), while for most hard X-ray flares and for the gamma-ray flares describe above the power law index $\gamma > 2$. This would indicate a synchrotron spectral index < -1, *i.e.*, a declining spectrum. In the model proposed by Ramaty and Petrosian (1973), where the flat portion of the spectrum is due to free-free absorption of synchrotron emission, the spectrum could remain flat out to higher frequencies. The spectrum could even rise as in the Inverse Compton model proposed by Kaufmann *et al.* (1990). Taking the middle ground, the extrapolation of the spectrum of large flares shown in Figure 2 would indicate an expected Submm-FIR flux as large as 10^3 solar flux units or 10^{-16} erg/(cm^2 s Hz). Such events, of course, would be rare, occurring, on the average, approximately once per month.

The gamma-ray flares observed by Compton-GRO and Gamma-1 mentioned above indicate emission of about 10^{-8} to 10^{-9} erg/(cm^2 s) above 100 MeV. Extending the analysis of Lu and Petrosian (1989) to higher frequencies and electron energies we can estimate the expected flux at $\nu \approx 10^{13}$ Hz. Such photons will be emitted by 100 MeV particles in a magnetic field of $B = 500$G. The yield of synchrotron radiation from relativistic electrons of energy E spiralling with a 45° pitch angle along a length L of the coronal portion of the loop will be $Y_s \sim 10(B/500\text{G})^2(L/2 \times 10^9\text{cm})E$, while the bremsstrahlung yield at gamma-ray energies when the electron reaches the photosphere will be $Y_b \approx 10^{-5}E \ln E$ (see for example, Petrosian 1985). This and the observed gamma-ray flux would imply an expected synchrotron emission at $\nu \sim 10^{13}$ Hz of about 10^{-16} erg/(cm^2 s Hz), which is similar to the above estimation based on the observed millimetric flux.

Note that the photospheric emission (black body at 6000 K) at 10^{13} Hz is 4.5×10^{-18} erg/(cm^2 s Hz) arcsec^2. Therefore, a source size and angular resolution less than 5 arcsec is needed for the flare emission to exceed the background (see Figure 1).

The *Gradual, Thermal Emission* at Submm wavelengths can be estimated based on the observed soft X-ray fluxes. The uncertainty here lies in the fact that thermal gyrosynchrotron and thermal bremsstrahlung are two possible mechanisms for emission in the radio and IR range. The soft X-ray observations yield values for the electron temperature ,T, and the emission measure, EM. At very low frequencies the optical depth will be larger than one. At these frequencies the spectrum will be proportional to ν^2. For $\nu > \nu_b^*$, the frequency where the optical depth is one, the spectrum of thermal bremsstrahlung radiation will be nearly flat [$\nu F(\nu) \propto \nu$], eventually joining the exponentially decreasing soft X-ray spectrum at 10^{18} Hz (see Figure 1). Gyrosynchrotron emission, when optically thin ($\nu > \nu_s^*$), will deviate from the Rayleigh-Jeans spectrum approximately as $\exp[-(\nu/\nu_{crit})^{1/3}]$ (see Petrosian 1983, and McTiernan and Petrosian 1984). It then follows that if $\nu_s^* \leq \nu_b^*$, gyrosynchrotron radiation will be less intense than bremsstrahlung at all frequencies, while if $\nu_s^* > \nu_b^*$, which is the case depicted in Figure 1, gyrosynchrotron emission will exceed bremsstrahlung for some range of frequencies above ν_b^*. For a more detailed discussion of this matter see Figure 2.22 and the related text in Harding, Petrosian, and Teegarden, 1984.) The exact range of frequencies where this occurs depends on the relative values of ν_b^*, ν_s^*, and ν_{crit}, which are functions of temperature, density, magnetic field, and size of the emitting plasma. Ignoring some slowly-varying logarithmic terms, we may write

$$\left(\frac{\nu_s^*}{\nu_b^*}\right) \approx 0.4 \left(\frac{B}{500\ \mathrm{G}}\right) \left(\frac{T}{10^8\ \mathrm{K}}\right)^{15/8} \left(\frac{10^{10}\ \mathrm{cm}^{-3}}{n}\right) \left(\frac{10^9\ \mathrm{cm}}{L}\right)^{1/2}. \quad (2)$$

so that for large flares with emission measure $EM \approx n^2 L^3$ exceeding 10^{51} cm^{-3} this ratio will be less than one and gyrosynchrotron radiation will be unimportant. In that case the surface brightness temperature will be given by $T_B = T(\nu/\nu_b^*)^{-2}$ which will be greater than the background brightness temperature if $T \geq 3 \times 10^7$ and $\nu < 70\,\nu_b^*$. For $\nu_b^* = 10^{10}$ Hz the gradual phase thermal emission would be detectable up to 10^{12} Hz, just barely into the submillimeter range.

Thus, we conclude that even though one can be optimistic about detecting impulsive phase emission from large flares into the Submm and FIR range, it appears difficult to detect thermal emission from the weaker and more common flares unless the plasma temperature and magnetic field are very high ($B > 10^3$ G, $T \geq 10^8$ K).

5. Discussion and Summary

I have described the relationship between the Submm and FIR emission and that at other photon energy ranges. The impulsive phase emission most likely will be dominated by synchrotron radiation of electrons accelerated to extreme relativistic energies. Extrapolation to higher frequencies of observed millimetric fluxes, a thick-target model calculation, and observed gamma-ray fluxes predict 10^{-16} erg/(cm^2 s Hz) of radiation in the 10^{13} Hz range from the largest flares. The flare brightness will then exceed the solar black-body brightness only in compact flares (angular simeq$\theta < 5''$ or linear size $L < 3500$ km). The thermal emission in the Submm-FIR range will most likely be dominated by free-free (*i.e.* thermal bremsstrahlung) emission which for an electron temperature of 3×10^7 K will have a brightness exceeding the 6000 K black body emission only below 10^{12} Hz.

One may wonder whether such observations of flares are needed when we already can predict the fluxes at these frequencies. In addition to the fact that we always must test theoretical predictions by observations, as is generally the case with new observations, some surprises may be in store for us. For example, the impulsive-phase emission at Submm-FIR may be comparable to the much larger white-light emission rather than millimetric radio emission. Or some other yet unknown mechanism may produce strong radiation in this range during the impulsive or gradual phases.

Even ignoring these possibilities, higher spatial resolution is possible in the Submm-FIR range as compared to very high energy gamma-rays which would be helpful in clarifying the acceleration and radiation site for relativistic electrons. Furthermore, higher-spectral-resolution observations and possible polarization measurements in the Submm-FIR range as compared to the X- and gamma-ray ranges can further clarify the emission mechanisms and set more rigid constraints on model parameters.

Acknowledgements

This work was partially supported by NASA NAGW 1976 and NSF ATM 90-11628.

References

Brown, J.C., Hayward, J. and Spicer, D.S.: 1981, *Astrophys. J. (Letters)* **245**, L91.
Dennis, B.R. and Zarro, D.M.: 1992, in press.
Dröge, W., Meyer, P., Evanson, P. and Moses, D.:1989, *Solar Phys.* **121**, 95.
Hamilton, R.J. and Petrosian, V.: 1992, *Astrophys. J.*, in press.
Harding, A.K., Petrosian, V. and Teegarden, B.J.: 1986, in E. Liang and V. Petrosian (eds.), *Gamma-ray Bursts*, AIP Conference Proceedings 141 (Stanford, CA), p. 115.
Kaufmann, P., Correia, E., Costa, J.E.R. and Zodi Vaz, A.M.: 1986, *Astron. Astrophys.* **157**, 11.
Kiplinger, A.L., Dennis, B.R., Frost, K.J. and Orwig, L.E.: 1984, *Astrophys. J. (Letters)* **287**, L105.
Kocharov, G.E., Kocharov, L.G., Kovaltsov, G.A. and Guelenko, V.G.: 1991, preprint. To be published in *Nuclear Astrophysics.*
Kundu, M.R. and Woodgate, B.: 1986, *Energetic Phenomena in the Sun*, NASA Conference Publ. 2439, chapter 3.
Kundu, M.R., White, S.M., Gopalswamy, N. and Lim, J.: 1992, preprint; see also *Bull. Amer. Astron. Soc.* **24**, 783.
Leach, J. and Petrosian, V.: 1983 *Astrophys. J.* **269**, 715.
Leach, J., Emslie, A.G. and Petrosian, V.: 1985, *Solar Phys.* **96**, 331.
Lee, T. and Petrosian, V.: 1992, *Bull. Amer. Astron. Soc.* **24**, 794.
Lu, E.T. and Petrosian, V.: 1988, *Astrophys. J.* **327**, 405.
Lu, E.T. and Petrosian, V.: 1989, *Astrophys. J.* **338**, 1122.
Miller, J.A. and Ramaty, R.: 1989, *Astrophys. J.* **344**, 973.
McTiernan, J.M. and Petrosian, V.: 1990, *Astrophys. J.* **359**, 524.
McTiernan, J.M. and Petrosian, V.: 1991, *Astrophys. J.* **379**, 381.
Neupert, W.M.: 1968, *Astrophys. J. (Letters)* **153**, L59.
Petrosian, V.: 1973, *Astrophys. J.* **186**, 291.
Petrosian, V.: 1981, *Astrophys. J.* **251**, 727.
Petrosian, V.: 1985, *Astrophys. J.* **299**, 987.
Petrosian, V. and McTiernan, J.M.: 1983, *Physics of Fluids*, **26**, 3023.
Petrosian, V. and McTiernan, J.M.: 1991, *Bull. Amer. Astron. Soc.* **23**, 1044.
Ramaty, R. and Petrosian, V. : 1972,*Astrophys. J.* **178**, 241.
Rieger E., Reppin, C., Kanbach, G., Forrest, D.J., Chupp, E.L., and Share, G.H.: 1983, Proc. 18th Internat. Cosmic Ray Conf., **4**, 79.
Rieger, E., Marschhäuser, H.: 1991, in R.M. Winglee and A.L. Kiplinger (eds.), *MAX 91/SMM Solar Flares, Observations and Theory*, Proc. MAX91 Workshop No. 3 (Boulder, CO), p. 68.
Vestrand, W.T., Forrest, D.J., Chupp, E.L., Rieger, E., and Share, G.H.: 1987, *Astrophys. J.* **322**, 1010.
White, S.M., Kundu, M.R., Bastian, T.S., Gary, D.E., Hurford, G.J., Kucera, T. and Bieging, J.H.: 1992, *Astrophys. J.* **384**, 656.